Results of High-Harmonic Fast Wave Experiments on NSTX*

D. W. Swain[1], J. R. Wilson[2], P. M. Ryan[1], R. I. Pinsker[3], M. D. Carter[1], D. Gates[2], G. R. Hanson[1], J. C. Hosea[2], R. Maqueda[4], T. K. Mau[5], J. E. Menard[2], D. Mueller[2], C. K. Phillips[2], S. A. Sabbagh[6], D. Stutman[7], J. B. Wilgen[1]

[1] *Oak Ridge National Laboratory, Oak Ridge, TN, USA 37831-8071*
[2] *Princeton Plasma Physics Laboratory, Princeton, NJ, USA*
[3] *General Atomics, La Jolla, CA, USA*
[4] *Los Alamos National Laboratory, Los Alamos, NM, USA*
[5] *University of California San Diego, La Jolla, CA, USA*
[6] *Columbia University, New York, NY, USA*
[7] *Johns Hopkins University, Baltimore, MD, USA*

Introduction

The NSTX (National Spherical Torus Experiment) facility located at Princeton Plasma Physics Laboratory has completed its first 5-month operational period, during which it achieved 1-MA plasma operation [1]. The major device parameters are $R_0 = 0.85$ m, $a \approx 0.67$ m, $\kappa \leq 2$, $I_p \leq 1$ MA, $B_0 \approx 0.25$ T (future upgrades to 0.5 T are possible). Typical ohmic pulses have a 200 ms duration with average densities in the 0.5 to 1 x 10^{19} m^{-3} range .

The ion cyclotron system is designed to be a major source for heating and current drive. It operates at a fixed frequency of 30 MHz, $\approx 16\omega_{ci}$ for the deuterium ion majority, and is designed to deliver up to 6 MW to the plasma. Calculations indicate that most ($\geq$ 90%) of the power will be absorbed by the electrons. It will be used to heat and drive current in the plasma; for low-β operation the driven current is peaked on axis, while for higher-β cases the peak in the driven current is off-axis (at $r/a \approx 0.6$) due to the higher electron absorption.

During planned operating scenarios, the rf heating and current drive will begin early in the pulse when the plasma is cold and tenuous; the inter-antenna phasing will have to be ~90° in order to have adequate absorption under these conditions. Later in the pulse, 6 MW of rf power could result in a plasma $\beta \geq 25\%$. In order to drive current efficiently in this regime, the inter-antenna phasing should be between 30° and 60°, where calculations indicate plasma current $\geq$ 300 kA could be driven. This scenario therefore requires that the inter-antenna phasing be able to be changed during the plasma shot in order to vary the amount of current driven by the system.

Description of the ion cyclotron system

The ion cyclotron launching system consists of 12 antennas mounted to the wall of the vacuum vessel, and subtending almost 90°toroidally. A picture of the 12 antennas (Fig. 1) shows the limiters of boron nitride that surround each antenna. Each antenna is covered by a single-layer, 50% transparent Faraday shield. The current strap is grounded at one end and driven at the other end [2].

The electrical setup that was used for initial operation is shown in Fig. 2, in which two transmitters were used to drive eight of the twelve antennas. The antennas were connected into four resonant loop circuits, with two loops driven by each transmitter. Phasing between transmitters could be set to drive the antennas either in 0πτ0 phasing (launching a power spectrum with a peak in k_{tor} at 9 m^{-1}), or 0π0π phasing (with peak $k_{tor} \approx 13$ m^{-1}).

* This research was sponsored by the Office of Fusion Energy, U. S. Department of Energy, under contract DE-AC05-96OR22464 with Oak Ridge National Laboratory managed by UT-Battelle and under contract DE-AC02-76CH03073 with Princeton Plasma Physics Laboratory.

Plasma loading

The effect of the plasma on the antenna characteristics was measured during the rf experiments. The forward and reflected power vs. time, measured on the generator side of the tuning stubs shown in Fig. 2, was translated to the junction of the resonant loop with the main transmission line. A circuit model that included inter-antenna coupling was used to relate the reflection coefficient at this junction to the intrinsic parameters of the antennas, namely the resistive loading *R'* (ohms/m) due to the plasma, and the change in the antenna inductance per unit length *L'*. The characteristics of the antennas with no plasma, obtained from comparison of measurements with the same circuit model, gave good agreement between the measurements and calculations in vacuum.

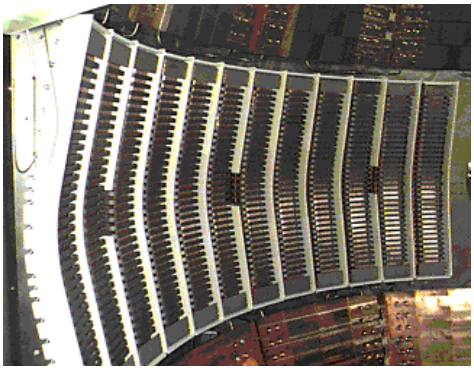

Fig. 1. NSTX antenna array

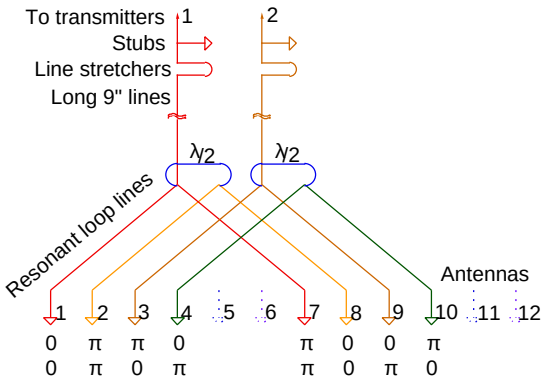

Fig. 2. Circuit schematic

Figure 3 shows the value of *R'* and *L'* calculated from the circuit model during a shot in which the plasma was limited on the inner wall. The outer gap (the distance from the front of the antenna BN limiters to the outermost unlimited flux surface) was swept from 12 cm to 4.5 cm during the 700 kW rf pulse. This shot used 0π0π phasing.

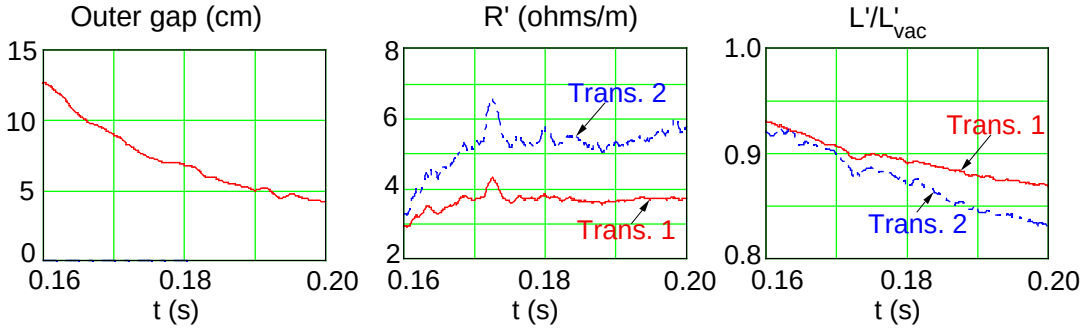

Fig. 3. Antenna loading and inductance change during a gap scan (shot 101544)

For the same shot, density profile measurements using a microwave reflectometer on the plasma midplane were obtained during the rf pulses. Profiles measured at 160, 170, and 195 ms are shown in Fig. 4. The vertical dashed lines indicate the location (with estimated error bars of ± 1 cm) of the outermost unlimited flux surface, based on magnetic equilibrium reconstructions. There is good agreement between the "edge" of the plasma determined from the magnetics and from the reflectometer data. The horizontal dashed line shows the lowest density that was directly measured by the reflectometer, which operated with a lower frequency of 6.5 GHz (O-mode launch) during the initial experiments.

Using the measured density profiles, plasma loading was computed using the FWLOAD [3] and RANT3D [4] codes. FWLOAD uses cylindrical geometry, RANT3D uses slab geometry with a more refined antenna model. Figure 5 shows a plot of measured and calculated loading vs. time for the same shot. The calculated loading shows much more variation during the gap scan

than the measurements. However, there is considerable uncertainty in the loading calculation, because the density profile below 0.5 x 10^{18}m^{-3} is not measured; extrapolations of the profiles are used to calculate *R'*, but the profile uncertainty introduces substantial uncertainties in the *R'* result.

One of the more interesting and unexpected behaviors during the experiment was the observation of the pronounced difference in *R'* for the two transmitters, as seen in Fig. 5. While often observed with current-drive phasing in other experiments, usually the calculated and measured values of *R'* are approximately the same with 0 or π phasing between straps. The asymmetry in measured plasma loading was observed on almost all rf shots.

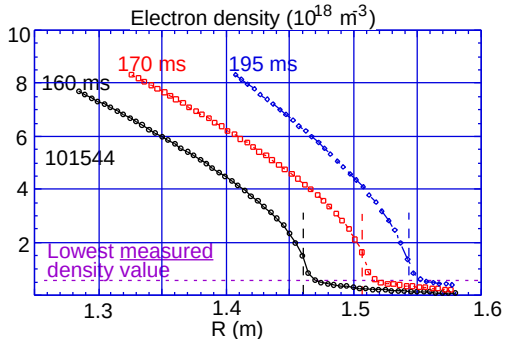

Fig. 4. Density profiles at three times (shot 101544)

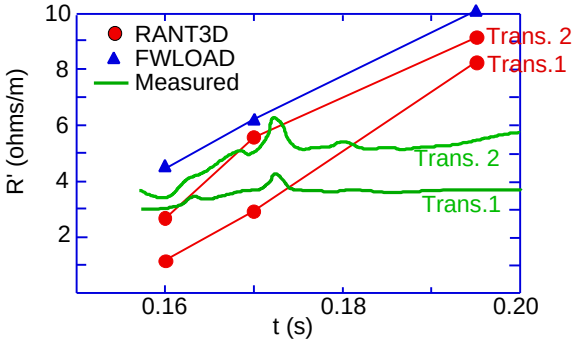

Fig. 5. Measured and calculated R' (shot 101544)

While it is possible that there is a systematic error in the measurements, the asymmetry may be a real effect. Calculations of the power spectrum radiated into the plasma by both the FWLOAD and the RANT3D codes indicate a significant asymmetry in the toroidal direction, which may explain the R' asymmetry. The asymmetry appears to be primarily due to the large pitch angle of the magnetic field at the antenna, which can be > 45° in NSTX. This has a profound effect on the toroidal symmetry of the launched power spectrum, as illustrated in Fig. 6. The plots show the radiated power spectrum calculated for shot 101544 at 170 ms. If the poloidal field is set equal to zero (left figure) the spectrum is symmetric, but if the actual value of B_{pol} is used the launched power is almost completely in one direction (right figure). The spectral asymmetry also is reflected in the power from each antenna. In RANT3D, a calculation of the integral of *Re*(**E•j**) along the radiating part of each antenna gives the power radiated. These show strong differences for the 160 and 170 ms cases, as shown in Fig. 5. However, the difference at 195 ms is small, in contradiction to the measurements.

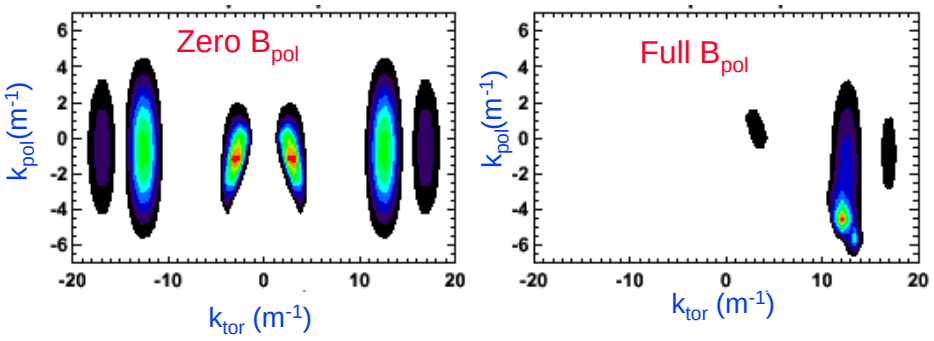

Fig. 6. Radiated power spectrum vs toroidal and poloidal wavenumber with zero poloidal field (left) and full poloidal field (right).

The decrease in *L'* as seen in Fig. 3 is in approximate agreement with that calculated by the replacement of the plasma edge with a simple metallic boundary. There is a small difference

seen in the measured values of L' for the two transmitters; however, this asymmetry is well within the error bars of the measurement. Code predictions for the NSTX rf system indicate that there may also be marked asymmetries in the mutual coupling between antennas in the presence of plasma This was beyond the ability of the initial rf diagnostics to measure, and will be the subject of future study.

Initial heating results

During initial high-harmonic fast wave (HHFW) experiments, up to 1 MW of HHFW heating power was coupled to the plasma for 50 ms during the current flattop phase, and up to 2 MW was coupled briefly. Results were obtained with both 0πτ0 and 0π0π inter-strap phasing. Figure 7 shows the change in plasma energy (obtained from EFIT analysis of the magnetic equilibrium) caused by the addition of ~1 MW of HHFW power. For these shots $I_p \approx 550$ kA, $\langle n_e \rangle \approx 0.6 \times 10^{19}$ m^{-3}, and $P_{OH} \approx 1.4$ MW. The 30% increase in energy is in agreement with $P^{1/2}$ L-mode confinement scaling.

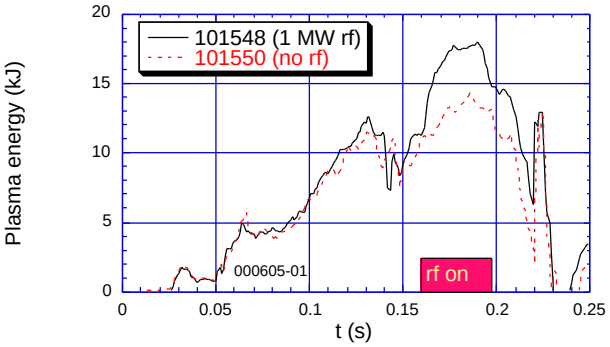

Fig. 7 Change in stored energy with 1 MW HHFW heating

Indications of electron heating in the plasma core have been observed by an array of filtered x-ray detectors. Analysis of this data is complicated by metal line emission, but modeling suggests an electron temperature rise from 0.8 to 1.2 keV early in the RF pulse.

Significant electron heating was only observed for 0π0π phasing (lower phase velocity) and not for 0πτ0 phasing. One explanation for this would be absorption by H minority ions. The H/D ratio in NSTX is estimated to be ≤ 10%. Calculations indicate that for H/D greater than a few percent, a hot ion tail (that could be formed by initial absorption by cold H ions) could absorb over 50% of the wave power. However, the fraction absorbed by ions is very sensitive to: (1) the toroidal velocity of the launched wave, increasing significantly for faster waves; (2) the temperature of the H ions, increasing as T_H (and hence. $k\ \rho$) is increased. A neutral-particle analyzer (planned for initial operation this fall) should help resolve this issue.

Plans for future operation

During the next phase of operation (scheduled to start in the summer of 2000), the HHFW system will consist of the full 12-strap fast-wave antenna array and six 2-MW rf sources, each source driving a separate resonant loop. The system will include six decouplers that will allow arbitrary phase differences between the transmitters. The goal is to deliver up to 6 MW of HHFW power to the plasma, and to be able to vary the inter-strap phasing during a plasma pulse in order to control both the heating and driven current in the plasma. In addition to the increase in the rf power, work will continue on the study of the power deposition in the plasma, and loading vs. plasma parameters. The NSTX HHFW system is exploring new ground, in which the combination of low field and high harmonic number, large values of $k\ \rho$, large values of B_{pol}/B_{tor}, and up to 40% β should lead to interesting and heretofore unexplored physics effects.

References

[1] M. Bell et al., "Physics Results from the National Spherical Torus Experiment", this conference.

[2] P. M. Ryan et al., "Design of the HHFW Heating and Current Drive System for NSTX," *Proc. 2nd Europhysics Top. Conf. on RF Heating and Current Drive of Fusion Devices*, Brussels, Belgium, European Physical Society, pp. 97, Jan. 20-23, 1998.

[3] J. Menard, "High-Harmonic Fast Wave Coupling and Heating Experiments in the CDX-U Spherical Tokamak", Ph.D. Thesis, Department of Astrophysical Sciences, Princeton University, June 1998.

[4] M. D. Carter, et al., “Three Dimensional Modeling of ICRF Launchers For Fusion Devices”, *Nucl. Fus.* **36**, p. 209, (1996)